

Controlling Tiny Multi-Scale Robots for Nerve Repair

Tad Hogg

HP Labs
Palo Alto, CA

David W. Sretavan

University of California San Francisco School of Medicine
San Francisco, CA

Abstract

We designed and evaluated multiagent control for microscopic robots (“nanorobots”) aiding the surgical repair of damaged nerve cells. This repair operates on both nerves as a whole, at scales of hundreds of microns, and individual nerve cell axons, at scales of about a micron. We match the robots to these sizes using a combination of microelectromechanical (MEMS) machines for the larger operations and nanorobots for operations on individual cells. Multiagent control allows accurate and rapid repair with such robots, with only modest computational and communication requirements for the nanorobots, a significant benefit due to their physical limitations. Our simulations, using physical parameters dictated by nerve biology and plausible nanorobotic capabilities, show how specific control choices lead to trade-offs in clinical outcome. Beyond the specific example of nerve repair treated here, multi-scale robots could aid a variety of medical and biological tasks involving both the large scale of organs or tissues and the microscopic scale of individual cells.

Introduction

Distributed control of large groups of robots allows rapid response to each robot’s local environment and overall coordination to accommodate robot failure as well as limited robot hardware capabilities. These issues are particularly relevant for proposed microscopic robots, with severe physical limits on available power, computation, and communication range. Such nanorobots, with sizes comparable to bacteria, could aid disease diagnosis and treatment since their size is well-suited for sensing and manipulating individual cells, and they can be deployed in sufficient numbers to simultaneously act on large cell populations [9, 18]. Although nanorobot fabrication is beyond current technology, the rapid progress in engineering nanoscale devices [7, 8, 16, 11, 25, 1] should eventually enable production of such machines. Effective use of these robots requires identifying suitable tasks and developing controls accounting for their physical properties and task environments, which differ considerably from those of larger robots. Medical applications provide a rich range of such tasks.

Many biological processes involve activities at molecular, cell, tissue and organ levels. Robotic interventions in these processes would ideally be able to sense and act at these different scales. This paper examines a multi-scale robot scenario in the context of nerve cell repair. The physical properties of the task environment and the use of robots of different sizes provide a novel domain for distributed control. In the following sections, we discuss nerve biology, protocols for

nanorobot-assisted axon repair, and simulations using physical parameters for mammalian nerves to illustrate nanorobot performance trade-offs.

Nerve Injury and Axon Biology

The nervous system governs our interaction with the external world and controls our sensory perception, muscle movement, and innate reflexes. Nerves are highly ramified throughout the body and trauma frequently results in nerve damage. Nerves range from $50\mu\text{m}$ to several millimeters in diameter, are up to a meter long and contain hundreds or thousands of axons. Axons, the elongated structures from nerve cell bodies with diameters of a micron or so, transmit information via electrical impulses. A nerve can contain axons signaling in different directions: *sensory* axons convey environmental input to the brain and *motor* axons send commands from the brain to the muscles. These two axon types, which tend to be somewhat, but not completely, segregated within a nerve, differ in diameter, membrane composition, and microtubule orientation.

Electrophysiological testing is a standard method of confirming axon function. A small external stimulation can trigger electrical conduction in axons and electrophysiologists routinely place small recording glass micropipettes into nerve cells without harming the cell. For instance, in retinal neurons, whose axons form the optic nerve, inserting an electric charge of 5nC into an axon initiates a signal [19]. Nanorobots injecting charge into an axon via small probes are likely to activate signals with less charge due to their direct contact with the axons, i.e., using currents in the picoampere range.

Axons in a nerve tend to maintain their topographic relationship, i.e., axons originating from neighboring nerve cells tend to remain close together, project to adjacent target cells, and serve similar functions. There is some mixing of axons within a nerve over lengths of centimeters. This mixing, or *topographic deviation*, makes it difficult to match segments of an axon from the same cell from just their physical position in the nerve when the segments are separated by long distances. Fortunately, axons express membrane chemicals with functionally closely related axons having similar levels of these molecules. These molecular expression levels could help identify functionally related axons over macroscopic distances along a nerve, as required for the repair procedure described below. In this paper, we use “neighborhood” to mean a group of axons of the same type (i.e., sensory or motor) that connect to adjacent sites. Deviation amount and neighborhood size vary among different nerves.

Although axons can bend without compromising cellular function, they can be damaged in trauma. Treating such

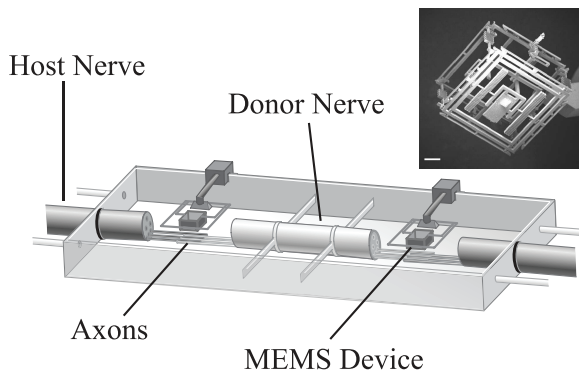


Figure 1: Repair task geometry. Graft nerve (center) replaces damaged portion of original host nerve (left and right). A MEMS device operates on the exposed axons in each junction. The diagram is not to scale. Typical graft nerve is 1cm long, with $100\mu\text{m}$ diameter. Axon diameter is $1\mu\text{m}$, with only a few shown in each junction. Junction width is $10 - 100\mu\text{m}$. Inset: photograph of an actual MEMS axon repair device seen from below, about 1mm^3 in volume.

injury requires restoring the ability of the axons to transmit signals. Effective treatment does not require signals to travel along *exactly* the same axons as before the injury. Instead, signals sent along axons within the same neighborhood will result in functionally acceptable results. However, axon types are important: sensory signals should not be sent along motor axons or vice versa.

Much ongoing research attempts to regenerate damaged axons using pharmacologic means [23, 14]. An alternative paradigm involves direct surgical manipulation of damaged axons using microelectromechanical systems (MEMS) devices [24]. This method uses MEMS devices for precise axon cutting, non-contact electrokinetic axon manipulation, and axon fusion in a surgery chamber shown in Fig. 1. Repair begins with removal of the damaged region of the host nerve. A healthy segment from a graft nerve is then brought in. Axons at the ends of the host and graft nerves are exposed using enzymes that remove nerve connective tissue. A pair of host and graft axon ends is then aligned and apposed to each other for electrofusion by the application of electric fields of $2-8\text{ kV/cm}$ across the membrane. This process fuses the membranes of the host and graft axons and allows signal propagation between them. The same surgical sequence is then applied to additional host-graft axon pairs. Experimentally, these repair steps have been achieved in cell culture [5, 24]. Alternatively, the small size of the nanorobots could allow them to fuse cell membranes chemically, as occurs in biology [6].

Repair occurs in fluids of physiological osmolarity. The temperature is maintained below body temperature of 37°C to reduce axon metabolism and potentially benefit axon survival. For clinical use, a surgery protocol should be able to repair the axons in an injured nerve within a few hours.

Nanorobot-Aided Axon Repair

Although current research aims for complete repair with only MEMS microdevices, using nanorobots for sensing,

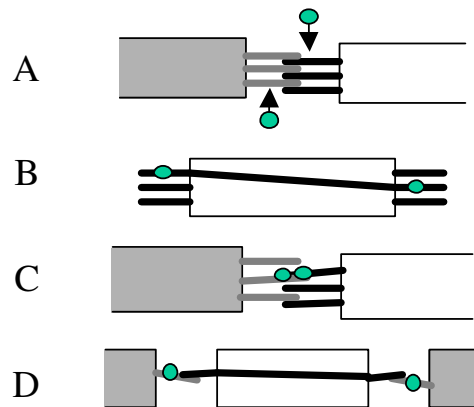


Figure 2: Schematic nanorobot tasks showing cross sections of the 3-dimensional operating environment. Nanorobots, circles; host axons, gray; graft axons, black: A) move to axons and determine their properties from membrane chemicals, B) map and identify the ends of graft axons, C) move host and graft axons together and fuse them, D) evaluate conductivity of repaired axon. Steps A and C show only one junction, and step B shows only the graft nerve.

manipulating, and testing axons could improve outcomes. Nanorobots are an attractive tool for axon repair since their size allows them to interact with and move individual axons. In this case, the MEMS device at each junction releases a population of nanorobots. Removing only about $10\mu\text{m}$ of connective tissue to expose the axons should be sufficient for the nanorobots, compared with $100\mu\text{m}$ needed if MEMS devices are used alone. Less removal of supportive tissue should allow better preservation of nerves, and faster healing as supporting tissue grows back.

We consider nanorobot capabilities well within likely hardware and medical safety limits [9]. Thus our control protocols are conservative and a mature nanorobot technology could likely perform better. The nanorobots use chemical sensors, based on specific receptors in their surface and similar to sensors used by cells to recognize each other. Once the robots are within a few microns of the axons, they can use such sensors to identify membrane chemicals by simply waiting to collide with the cells via Brownian motion. Such collisions are frequent, giving many chemical sensing opportunities [2]. At the relevant slow speeds, collisions do not damage cells or robots. The robots must also detect electrical signals in axons.

We require nanorobot communication over about $10\mu\text{m}$ with other nanorobots, and over somewhat longer distances with the MEMS device. Ultrasound is a reasonable modality for this communication, and readily handles the modest bit rates required for our control protocol. With a known acoustic output, measuring the intensity of the received ultrasound also allows estimating the range of nearby nanorobots.

For actuators, the robots require means of locomotion such as cilia. Unlike larger robots, nanorobot motion is dominated by viscosity [20] and has noticeable Brownian motion: in time t , measured in seconds, robots are randomly moved with a root-mean-square displacement of about $\sqrt{t}\mu\text{m}$ and change orientation by about $1.6\sqrt{t}$ radian. The

robots must inject charge into an axon to trigger electrical conduction, and fuse membranes either electrically or chemically. Power estimates for nanorobot motion and communication [9] indicate these activities require about 1000pW per robot over the duration of the repair. Nanorobots could get power from the environment [9]: e.g., glucose and oxygen added to the fluid, at concentrations similar to that of arterial blood, or ultrasound from the MEMS device.

The MEMS devices must transport nanorobots to the junctions, release them among the axons, and retrieve them at the end of surgery. In addition, the MEMS devices must communicate with their nanorobots and be able to interact mechanically and electrically with the nerve as a whole.

The remainder of this section describes a control protocol exploiting the capabilities of the different robot sizes.

Deploying Nanorobots to the Axons

Axons will be distributed throughout the cut cross section of the nerve. Nanorobots at the junction perimeter need about 2500s to diffuse $50\mu\text{m}$ by Brownian motion, so we use active motions toward the axons (Fig. 2A). A plausible speed of $1000\mu\text{m/s}$ (comparable to the flow speed in small blood vessels) allows a nanorobot to cover the $50\mu\text{m}$ to axons at the center of a junction in about 50ms, during which time Brownian motion is insignificant. Using a distribution of robot speeds, based on the roughly circular junction geometry, this active motion places robots throughout the junction. They then wait as Brownian motion moves them to nearby axons to which they then attach. This diffusion requires only a few seconds to move the few microns to a nearby axon. This deployment protocol does not require robot coordination, thereby avoiding communication power use. While the protocol does not guarantee every axon has a robot, with a sufficient number of robots (e.g., 10 times the number of axons), each axon is likely to have at least one.

After reaching the axons, robots use short-range communication to check for other robots attached to the same axon. These robots, each with a unique identifier, select one of them to serve as the identifier for the axon itself.

Sensing: Identifying Axon Properties

The nanorobot attached to an axon tests if it is viable, and hence worth repairing (for host axons) or useful for repair (for graft axons). Viable axons can be identified by using the MEMS device and nanorobots for stimulation and recording, respectively. Macroscopic electrodes from the MEMS device stimulating the host (or graft) nerve activate every viable axon within the nerve. Nanorobots attached to those axons detect the signal and communicate their identifiers to the MEMS device. Robots not responding are not attached to a viable axon and will not participate in the repair.

From membrane molecule concentrations, the nanorobot identifies its axon's functional type and neighborhood position. Such sensing could use antibody based detection systems or the recognition of specific molecules by receptor proteins integrated into nanorobots.

Using short range communication each robot determines the identifiers of robots on adjacent axons in the junction within a specified distance d . This communication consists

of just the robot identifier, and received intensity allows estimating the range of the sending robot. As a control design choice, larger values of d provide more potential repair connections but also require more power for communication and axon motion. Reasonable values will be a few times the spacing between neighboring axons, i.e., $\approx 10\mu\text{m}$. Information on axon properties and robot identifiers amount to a few hundred bits and can be communicated acoustically to the MEMS device: e.g., in less than a millisecond using 10MHz ultrasound.

Matching Axon Ends Within the Graft Nerve

The graft nerve is compliant and may twist a bit. To ensure correct joining of the two ends of a host axon using a graft axon segment, the two ends of the same graft axon must be identified. This identification can again take advantage of electrical conduction along axons (Fig. 2B) using nanorobots to stimulate one axon at a time. A nanorobot attached to one end of a graft axon can inject sufficient charge into the axon to induce self-regenerative electrical conduction. Among the nanorobots at the other end of the graft nerve, nanorobots attached to the same axon will detect a signal. The successive stimulation of individual graft axons gives a complete mapping of the corresponding ends at the opposite side of the graft nerve.

Since direct communication between nanorobots on opposite sides of the graft nerve is not feasible, we use the MEMS devices to aid this process. One suitable protocol has the MEMS device at the left junction go through its table of identifiers for robots attached to graft axons and serially broadcast them. The nanorobot matching the identifier induces a signal in its axon. Conduction velocity is 1–100 m/s so the signal reaches the other end of the graft within 10ms. The robot on the right end of the stimulated graft axon receives the signal, and broadcasts its identifier to the MEMS device at that junction. Waiting, say, 100ms between broadcasting successive identifiers allows mapping the ≈ 1000 connections through the graft in a few minutes.

Planning The Repair Sequence

Finding an appropriate repair sequence from the collected axon properties is a computational search problem, which could use computational resources outside the surgical area. The repairs, i.e., host to graft connections at each junction, should connect the same type of host axon (e.g., sensory to sensory) and maintain axon neighborhoods. The distances axons need to be moved for fusion should be minimized, while ensuring many axons can be repaired in a short time.

The treating physician can specify the relative importance of the search criteria. For instance, the search could favor finding a few connections with minimal mismatch even at the expense of larger average error, or not repair axons with a large estimated mismatch, or give priority to one type of axon, sensory or motor. This computational flexibility and the use of cell-specific information collected over macroscopic distances, is a key benefit of multi-scale robots for medicine. In addition, communicating via the MEMS devices, the physician could adjust or halt the nanorobot operations based on their reports on the progress of the surgery.

With many axons and the mix of somewhat conflicting repair criteria, a complete search over all possible repairs could be computationally prohibitive. Instead, as an illustration, we consider a rapid greedy search giving priority to connections involving the least mismatch according to the available neighborhood information. To make the repair assignments, we start with all axons considered as “unused” and eliminate from the table any identified as not functional. For each host axon h , consider its nearby unused graft axons $\{g_1, \dots\}$. Next, at the opposite junction, consider the set of unused host axons $\{h_1, \dots\}$ found to be near at least one of those graft axons. From among these host axons, select the one h' of the same type as h and with the closest positional identity molecular markers. Then connect these host axons using one of the available graft axons close to both these host axons, and mark this graft and the hosts as used. Repeat until all host axons have assigned connections, or no further connections are available. This procedure produces a set of proposed connections without backtracking. The result is a list of repairs, i.e., host to graft axon connections, in each junction. The MEMS devices then broadcast the list to the nanorobots to initiate axon repair.

Moving and Fusing Axons

The robots instructed to join two axons must move them together and fuse their membranes (Fig. 2C). To guide the motion direction, acoustic ranging bursts between robots on the two axons can determine whether they are moving closer. Since isolated axons are fairly pliable, the fluid viscosity is the main resistance to moving axons. Thus a $10\mu\text{m}$ length of axon has about ten times the drag of a single $1\mu\text{m}$ robot. Using about 1pW a robot could move such an axon at a speed of $100\mu\text{m/s}$, hence positioning the host and graft axons together within about 0.1s , for repair assignments based on axons within $10\mu\text{m}$ of each other. Thus, even with serial motions, robots could repair 1000 axons in a few minutes.

Evaluating Repair and Nanorobot Retrieval

A key benefit of using nanorobots is the possibility of testing functionality of repaired axons. A procedure similar to that described above using electrical conduction to match axon ends in the graft nerve can determine whether the repair of a specific pair of axons is successful (Fig. 2D). The signal would be induced on the host axon in one junction and detected on the corresponding host axon in the other junction.

At the end of the entire repair procedure, the nanorobots will be removed via reliable recapture procedures including following a signal back to the MEMS device. The use of engineered nanorobot surface coatings [10] should prevent inflammation or immune system reactions during the repairs. Alternatively, if nanorobots have longer-term biocompatibility [10], they could aid or monitor the healing process with additional control protocols. The nanorobots can also record their operations and sensor values, providing detailed documentation of the procedure at the level of individual cells.

Simulated Robot Performance

To quantify the behavior of the MEMS and nanoscale devices, we simulate a typical case of the repair protocols de-

scribed above, in a $100\mu\text{m}$ -diameter nerve containing 1000 axons, each with $1\mu\text{m}$ diameter. We use 10^4 nanorobots per junction, each $1\mu\text{m}$ in diameter. We suppose the axons are distributed uniformly through the nerve cross section, only half are viable, and sensory or motor axons are equally distributed within the nerve.

The quality of repair outcome depends on how well information obtained by the nanorobots allows matching up the ends of the host axons in the two junctions. As the relevant biological properties of nerves are not yet well-characterized, we use the following simple models. The first property is the amount of topographic deviation, i.e., mixing of axons that started out as neighbors, between the two ends of the host nerve and in the graft nerve. We model this deviation with a parameter σ . Specifically, for each axon (host or graft), we assign a random point (x, y) within the nerve cross section to be the location of its left end. We then set the location of its right end to be $(x', y') = (x + \delta x, y + \delta y)$ where δx and δy are $N(0, \sigma)$ random variables, i.e., normally distributed with zero mean and standard deviation σ . Any global twists in which groups of neighboring axons are moved together we suppose are compensated for by overall twists of the graft when it is positioned. Such global adjustments are well-suited to the larger-scale manipulations possible with the MEMS device.

The second property is how well molecules on axon membranes allow matching up axons over centimeter distances along a nerve. We suppose each axon membrane has a fixed pattern of positional identity chemicals along its length, e.g., obtained from chemical gradients during nerve development. If these chemical concentrations were distinct enough to identify individual axons, then measuring the concentrations on host axons in the two junctions would allow perfect matching of the ends of host axons connected to each other before the damage. Although axons have such molecular positional identifiers, it is not yet known whether they can identify unique axons. Instead, we suppose the chemicals give some, but not necessarily perfect, information for matching axons. In the simulation, we characterize the quality of this matching by a parameter Σ . Continuing with the above example of an axon given locations $H = (x, y)$ and $H' = (x', y')$ in the left and right junctions, let axon h in the left junction be the best match to axon H' inferred from the membrane properties. We quantify the quality of this inference by associating with H' the difference in physical locations between the best inference h and the actual best match H in the left junction. As a simple model, we take the difference in each coordinate of the locations to be a $N(0, \Sigma)$ random variable. A value $\Sigma = 0$ corresponds to correctly determining how axons match up from their chemical signature, while Σ considerably larger than the diameter of the nerve means the molecules give no useful information.

In summary, σ characterizes a *physical* property, the topographic deviation in a nerve, while Σ characterizes the *inference accuracy* with which corresponding axons can be matched up via the chemical markers on their surfaces. Values of σ and Σ for nerves are not well characterized at present, so we consider a plausible range of values based on current biological measurements of nerve structure.

In the simulation, nanorobots move to the axons as de-

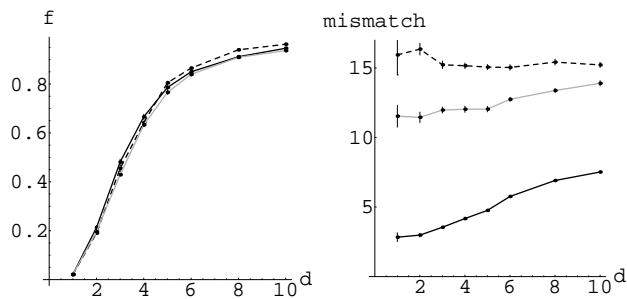


Figure 3: Simulated repair performance vs. the distance d robots examine for neighbors. The curves show nerves with different topographic deviations: $\sigma = 2\mu\text{m}$ (solid), $\sigma = 10\mu\text{m}$ (dashed), $\sigma = 10\mu\text{m}$ in host and $\sigma = 2\mu\text{m}$ in graft (gray). Neighborhood accuracy is $\Sigma = 5\mu\text{m}$. (left) fraction f of possible repairs made; (right) mismatch score of the repair. Each point is the average from 10 simulated trials, with error bars for the standard error of the mean (often smaller than the size of the plotted points). Distances are in microns.

scribed above, subject to Brownian motion. Each robot determines its axon’s type, functionality and neighborhood relationships and identifies robots within a specified distance d . Using this information, the simple search described above produces a repair allocation, i.e., a list of host to graft connections at each junction. This simulation assumes such repairs are then performed as specified. Repair errors could be modeled as an additional failure probability.

This simulation, although simplified, allows the comparison of various design choices for nanorobots. One clinically-relevant performance measure is the fraction f of functional host axon ends that are reconnected through the graft to host axons of the same type. Another measure is how well-matched the reconnected axons are. Specifically, consider a host axon end H in the left junction originally connected to host axon end H' in the right junction, but connected by the repair to axon end h' . We define the *mismatch* of this repair as the physical distance between H' and h' . The overall repair mismatch is the average value of the mismatch for each repaired host axon. A small mismatch means axons are reconnected to close neighbors. This average is only one possible clinically relevant measure: another could be the number of connections made within neighborhoods since those should function about as well as restoring the original connections. How much mismatch is tolerable for useful functional outcomes is an important open question. The simulation also provides engineering performance measures, such as the average distance the robots move to reach axons, the distance axons are moved to contact fusion partners, and the number of bits and distances over which they communicate. These measures quantify the required robot capabilities, e.g., power use.

Fig. 3 shows how increasing the distance d over which a nanorobot’s fusion partners are selected repairs more axons, but also increases the mismatch between the repaired and original host axons unless topographic deviation is large. This gives a clinical trade-off: is it better to have a few axons reconnected with little or no mismatch, or have more ax-

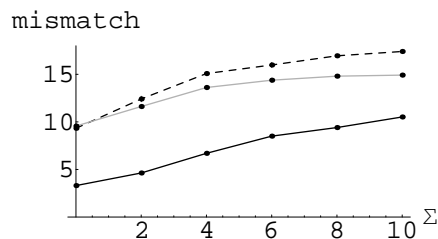


Figure 4: Average repair mismatch with $d = 10\mu\text{m}$ for $\sigma = 2\mu\text{m}$ (solid), $\sigma = 10\mu\text{m}$ (dashed) and $\sigma = 10\mu\text{m}$ for the host and $2\mu\text{m}$ for the graft (gray), as a function of Σ , the error range for matching axons. Each point is the average from 10 simulated trials, with error bars for the standard error of the mean smaller than the plotted point sizes. Distances are in microns.

ons reconnected but with larger errors? This trade-off arises because with small d , connections are only among nearby functional hosts, so the few connections that can be made tend to be among hosts with both ends functional allowing for zero-mismatch connections when the neighborhood information is accurate. With larger d , many connections involve hosts where only one side is functional, hence the smallest possible mismatch is at least the typical spacing between neighboring axons of the same type. The results also show an engineering consequence of increasing d : greater distances over which the nanorobots move axons and communicate requires more power. The simulations show that larger topographic deviations σ in host and graft nerves lead to worse performance. Using graft nerves with inherently low σ somewhat improves the outcome.

Fig. 4 illustrates another aspect of performance: the more accurately robots can infer correct axon match up from molecular markers, the smaller the matching error in the repaired connections. Thus the simulation quantifies how better biological understanding of the positional identity molecules in axon membranes improves repair.

We also considered limited repair resources. For example, if the graft is damaged during harvesting, resulting in fewer viable axons, or the number of functional host axons is unexpectedly high, there will not be enough graft axons to connect all the functional hosts. Alternatively, if the number of robots in each junction is not sufficient to ensure most axons have at least one robot, many functional axons will be, in effect, invisible to the repair procedure. In either case, the mismatch distance is similar to that discussed above, with a proportionate reduction in the fraction of repaired axons.

This simulation demonstrates the benefit of supplementing the MEMS devices with nanorobots. Without the nanorobots, or some other means of determining the type, functionality, and neighborhood information of individual axons as well as connectivity through the graft, the MEMS devices would have to select repairs based only on rough spatial location. With the parameters used here, such selection results in 75% of the repairs reconnecting either nonfunctional axons or sensory to motor host axons. The MEMS devices acting alone would also require more time to complete repairs and face possible tangling of axons due to the required removal of more supporting tissue.

Discussion

This paper describes distributed multi-scale control for axon repair. The simulation outcomes are not sensitive to plausible parameter variation and hence likely give order-of-magnitude clinically-relevant guidelines for repair time and accuracy. Further tuning of the control protocol requires better characterizations of biophysical axon properties, which nanorobots as research tools could help determine. An important extension is evaluating robustness against failures to help access the safety of nanorobot use in medicine.

Microscale physics emphasizes different control issues than those of larger robots [21]. For instance, perception, using chemical sensors, is algorithmically simpler than computer vision or sonar interpretation used for larger robots. At short distances, Brownian motion allows rapid random search in the environment without power use. Instead of path planning and complex team role negotiation, we need algorithms exploiting microphysics to coordinate robots and allow for their limitations, e.g., on power, communication range and computational capacity. Such algorithms emphasize reactive control [4, 13] based on patterns of sensory inputs, and utilizing environmental markers [15]. Stochastic analysis of collective behaviors [12] from algorithms using alternate combinations of nanorobot capabilities could demonstrate different ways to achieve a given task, thereby giving useful trade-offs for future hardware development.

Tiny multi-scale robot systems are likely to be useful in other biological research and medical contexts. Nanorobot populations can interact individually with many cells, while larger devices provide coordination over longer distances, more power and computational capability, and manipulation of larger biological structures. More generally reconfigurable [3, 22] and fractally-structured [17] robots could dynamically adapt to various scales as needed. Possible applications include vascular microsurgery, endoscopic diagnosis and therapy, as well as cancer detection and treatment in vivo. Thus control protocols for multi-scale robots provide a basis for extending multiagent systems to applications in a variety of medically-relevant microenvironments.

Acknowledgments

We thank R. Freitas Jr and L. Rosen for helpful comments.

References

- [1] Yaakov Benenson, Binyamin Gil, Uri Ben-Dor, Rivka Adar, and Ehud Shapiro. An autonomous molecular computer for logical control of gene expression. *Nature*, 429:423–429, 2004.
- [2] Howard C. Berg. *Random Walks in Biology*. Princeton Univ. Press, 2nd edition, 1993.
- [3] Hristo Bojinov, Arancha Casal, and Tad Hogg. Multiagent control of modular self-reconfigurable robots. *Artificial Intelligence*, 142:99–120, 2002. Available as arxiv.org preprint cs.RO/0006030.
- [4] Rodney A. Brooks. New approaches to robotics. *Science*, 253:1227–1232, September 13 1991.
- [5] W. Chang, C. Keller, and D. Sretavan. Precision MEMS nanocutting device for cellular microsurgery. In *ASME Intl. Mechanical Engineering Congress (IMECE2004-61670)*, 2004.
- [6] Elizabeth H. Chen and Eric N. Olson. Unveiling the mechanisms of cell-cell fusion. *Science*, 308:369–373, 2005.
- [7] C. P. Collier et al. Electronically configurable molecular-based logic gates. *Science*, 285:391–394, 1999.
- [8] H. G. Craighead. Nanoelectromechanical systems. *Science*, 290:1532–1535, 2000.
- [9] Robert A. Freitas Jr. *Nanomedicine*, volume 1: Basic Capabilities. Landes Bioscience, Georgetown, TX, 1999. Available at www.nanomedicine.com/NMI.htm.
- [10] Robert A. Freitas Jr. *Nanomedicine*, volume 2A: Biocompatibility. Landes Bioscience, Georgetown, TX, 2003. Available at www.nanomedicine.com/NMIIA.htm.
- [11] J. Fritz et al. Translating biomolecular recognition into nanomechanics. *Science*, 288:316–318, 2000.
- [12] Aram Galstyan, Tad Hogg, and Kristina Lerman. Modeling and mathematical analysis of swarms of microscopic robots. In P. Arabshahi and A. Martinoli, editors, *Proc. of the IEEE Swarm Intelligence Symposium (SIS2005)*, pages 201–208, 2005.
- [13] Brosl Hasslacher and Mark W. Tilden. Living machines. In L. Steels, editor, *Robotics and Autonomous Systems: The Biology and Technology of Intelligent Autonomous Agents*. Elsevier, 1995.
- [14] Z. He and V. Koprivica. The Nogo signaling pathway for regeneration block. *Ann. Rev. Neurosci.*, 27:341–368, 2004.
- [15] Owen Holland and Chris Melhuish. Stigmergy, self-organization and sorting in collective robotics. *Artificial Life*, 5:173–202, 1999.
- [16] Joe Howard. Molecular motors: Structural adaptations to cellular functions. *Nature*, 389:561–567, 1997.
- [17] Hans Moravec. *Mind Children: The Future of Robot and Human*. Harvard University Press, Cambridge, MA, 1988.
- [18] NIH. National Institutes of Health roadmap: Nanomedicine, 2003. Available at <http://nihroadmap.nih.gov/nanomedicine/index.asp>.
- [19] M. C. Peterman et al. The artificial synapse chip: A flexible retinal interface based on directed retinal cell growth and neurotransmitter stimulation. *Artificial Organs*, 27:975–985, 2003.
- [20] E. M. Purcell. Life at low Reynolds number. *American Journal of Physics*, 45:3–11, 1977.
- [21] Aristides A. G. Requicha. Nanorobots, NEMS and nanoassembly. *Proceedings of the IEEE*, 91:1922–1933, 2003.
- [22] B. Salemi, W.-M. Shen, and P. Will. Hormone controlled metamorphic robots. In *Proc. of the Intl. Conf. on Robotics and Automation (ICRA2001)*, 2001.
- [23] M. E. Schwab. Repairing the injured spinal cord. *Science*, 295:1029–1031, 2002.
- [24] D. Sretavan, W. Chang, C. Keller, and M. Klot. Microscale surgery on axons for nerve injury treatment. *Neurosurgery*, 57(4):635–646, 2005.
- [25] Ron Weiss and Thomas F. Knight, Jr. Engineered communications for microbial robotics. In *Proc. of Sixth Intl. Meeting on DNA Based Computers (DNA6)*, 2000.